Study of the micro-pin fin heat sink with MEPCM suspension and different types of PCMs: A Comparative Study

Hind Lafta Tbena [1] ⓘ

Abstract

In this paper used a microencapsulated phase change material (MEPCM) suspension and phase change materials (PCMs) in a micro-pin fin heat sink (MPFHS) with three types of fins (circular, triangular and square) are Numerically investigated. The MEPCM suspension used consists of microcapsules composed of PCMs n-octadecane and RT44, and shell materials used poly-methyl-methacrylate (PMMA) and poly-alpha-olefin (PAO). This capsules are suspended in different pure fluids pure oil, pure water and ethylene-glycol at a concentration of (0-20)%. Also, the phase change materials (PCMs) used represented by n-octadecane and RT44. The results obtained display that used MEPCM suspensions as a coolant fluid in micro-pin fin heat sinks in place of pure fluid leads to improved cooling performance of micro-pin fin heat sinks compared with used phase change materials (PCMs) only. Also, unfinned heat sink gives lower pressure drop and high rate of heat transfer coefficient compared with all types of fins used.

Keywords—Numerical investigation, Heat sinks, Micro pin fin heat sink, Phase change materials, Electronic cooling, Microencapsulated phase change materials.

1 Introduction

The technology of micro-pin fin heat sink has been progressively used to improve highly competent cooling device heat sinks and remove heat generation for small areas. Cooling fluids used in micro pin-fin heat sinks are represented by pure fluids or suspensions of indifferent compositions and concentrations. MEPCMs suspension may be used to advance the thermal enhancement of micro pin-fin heat sinks due to its ability for store and release large quantities of heat in devices. Many researchers have studied the performance of heat sinks with MEPCMs and PCMs. (Sabbah et al., 2009) the application of microencapsulated phase change material suspensions in fluid heat transfer to enhance the efficiency of micro-channel heat sinks is being studied numerically. A three-dimensional symmetrical model was utilized to create the suspensions flow and heat transfer. Phase change materials (RT44) which have a predetermined range of solidification and melting temperatures are contained in MEPCMs. The heat flux applied to the base is (100-500) W/cm^2 5.1 mm in width, 1.5 mm in height, and 10 mm in length make up the micro-channel heat sink.

Hind Lafta Tbena
hindlafta88@gmail.com

[1] Mechanical Engineering Department, College of Engineering, Thi-Qar University, Thi-Qar, Iraq

The 25 equally spaced of rectangular channels, each measuring 100 μm in width, 500 μm in depth and 10 mm in length make up the micro-channel heat sink. The results specified that, the latent heat effect and micro-mixing respectively improved the specific heat capacity, thermal conductivity and effectiveness of fluid because used microencapsulated. (Mehravar & Sabbaghi, 2014) the effect of microencapsulated phase change materials (MEPCMs) suspension on temperature of the cold and hot fluids for MEMS based heat exchanger by using latent heat through methods used represented with thermal energy storage are numerically studied. The properties of MEPCM and pure water have been considered dependent on temperature. Different volumes fractions of MEPCM slurry used and CFD software Fluent. Their results revealed that, at volume fraction 25% using of MEPCMs signs to improvement in fluid temperature. For hot fluid, the temperature increase can reach up to 23.5%. Furthermore, the temperature drop for cold fluid drops to 9%. (Arshad, Ali, Yan, et al., 2018) studied the effect of passive cooling for electronic devices by using the phase change material on the base heat sink. The values of heat flux applied to the heat sink base are (0.79 kW/m^2) to (3.17 kW/m^2) used for the pin-finned heat sinks selected with the pin thickness of 1, 2, and 3 mm. They used four values of volume fractions 0, 0.33, 0.66, and 1 for the amount of PCM emptied in all arrangements of heat sinks. Also, they used PCM (n-eicosane) and full in arrangement of heat sink which is made from aluminum. The results indicated that the phase duration of latent heat decreases with increasing value of input heat flux. Also, the maximum enhancement ratio of 4 is obtained in the case of a heat sink fully filled with the PCM at two values of the set point temperature (45 and 55)°C. Also, they found that, used a square pin fin heat sink with a thickness of (2*2) mm^2 and PCM (n-eicosane) at ψ = 1 gives the best heat transmission characteristics**.** (Hasan & Tbena, 2018) the phase-change material of the micro-channel heat sink was studied numerically. At varying ambient temperatures four phase change materials used (p116, RT41, paraffin wax and n-eicosane) and air have been employed as cooling media in various types and configurations. The results demonstrated that, improving the cooling performance of a micro heat sink can be achieved by utilizing phase change materials in micro-channel heat sinks with various configurations. (Fayyaz et al., 2022) experimentally studied of different combined effect of heat sink configurations and nano-enhanced phase-change material (NePCM) for cooling electronic devices. Aluminum used for the pin fin heat sink material, and RT-42 used as a nanoparticle for the phase-change material (PCM) at concentrations of 3 wt% and 6 wt%. Different heat sink configurations used against the fixed volume fraction of the fins, such as square, triangle, and circular pin fins. The results showed that the square configuration has the maximum heat transfer, both with and without PCM. When RT-42 was used as PCM, square pin fins showed a maximum base temperature reduction of 24.01%. At 6 weight percent of NePCM, the maximum base temperature of a circular pin fin dropped by 25.83%.

This paper numerically investigated a micro-pin fin heat sink (MPFHS) with PCMs and MEPCM suspensions consists of different base fluids, different core and wall materials of micro capsules. In addition to the fins with three different shapes used unfinned heat sink, are studied in order to compare geometrical parameters and coolant types.

2   Micro Pin Fins and Micro -Channel Heat Sinks

Micro heat sink which has pins that extends from its base is called micro-pin fins heat sink (MPFHS). This pin fins can be cylindrical, triangular or square shaped (Hasan & Tbena, 2018) as can be seen in fig.1. These types of pin fins heat sink are by far one of the most common types of heat sink available in the markets. A second type of the HS for fin arrangement in the shape straight fins with a hydraulic diameter ranging from (10 to 1000) μm is called micro-channel heat sink (MCHS). The straight fins in MCHS are not parallel to each other but in different arrangement. In this type of fins benefit from the full length of the heat sink. The straight fins are spaced from one to another at equal distances. In general, the greater surface area of the heat sinks, the better it will be when it does its work. The idea of heat sink with pin fins is an attempt to collect as much surface space as possible for the specified size. The performance of the pin fin (MPFHS) is greatly better than the straight fins (MCHS) when used in the intended applications where the flows of fluid is axially along the instead of touching it only tangentially across the pins (Arshad, Ali, Khushnood, et al., 2018).

3 Problem Description

The dimensions of the micro-pin fin heat sink are 20 mm in length, 200 µm in width, and 100 µm in height. The physical models with three fin geometries examined for the micro-pin fin heat sink are displayed in Fig. 1. There are 39 fins in a micro-pin fin heat sink, which come in three different shapes: square, triangle, and circular. The staggered configuration of all fins with the same height of 75 µm and base dimensions of $W\_F=D\_F = 25$ µm is preferred over the inline configuration for heat transfer (Soodphakdee et al., 2001) The values of fins spacing are sx = 8.5 µm and sz = 8.5 µm. This model applied conjugated heat transfer and developed flow.

a- Unfinned heat sink

b- Heat sink with circular fins

c- Heat sink with triangular fins
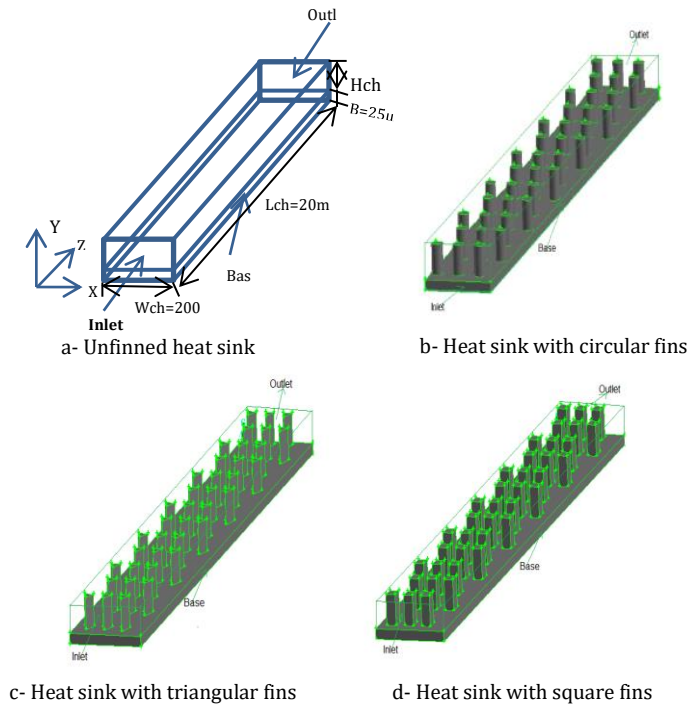
d- Heat sink with square fins

Figure 1: schematic of micro pin fin heat sink with (circular, triangular and square) fins and unfinned heat sink

4 Properties of the Microcapsules

MEPCM capsules consist of a PCM core and wall surrounding it. The wall can accommodate changes in space volume caused by a solid/liquid phase transition with satisfactory flexibility. A single particle of MEPCM is shown in Figure 2 to consists of two parts: outer polymer shell and inner PCM as well as between solid and liquid PCM moving interface.

The average diameter of MEPCM particles under study is 5µm. Core materials n-octadecane and RT44, shell materials poly-methyl-methacrylate (PMMA) and poly-alpha-olefin (PAO) are investigated. For every single particle of MEPCM, the study's core material (PCM) makes up roughly 70% of its volume. While the requirements for MEPCM can be determined by taking into account the properties of its various components, the core and wall materials have different properties. The microcapsules specific heat and density were calculated using mass balance and energy separately (KENISARIN & MAHKAMOV, 2007).
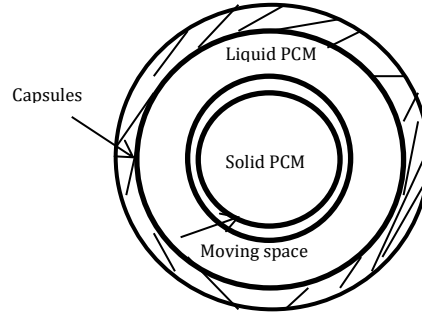
Figure 2: A single particle of MEPCM

5 Numerical Model

5.1 Governing equations

Three-dimensional continuity equation, momentum equations, and energy equation serve as representations of the governing equations for both suspension and pure fluids. The following notations can be used to express the governing equations (Agrawal & Dewangan, 2013), (Hasan, 2016).
The continuity equation:

$$\frac{\partial u}{\partial x} + \frac{\partial v}{\partial y} + \frac{\partial w}{\partial z} = 0 \qquad (1)$$

Momentum equations:

$$u\frac{\partial u}{\partial x} + v\frac{\partial u}{\partial y} + w\frac{\partial u}{\partial z} = -\frac{1}{\rho}\frac{\partial \rho}{\partial x} + \frac{\mu}{\rho}(\frac{\partial^2 u}{\partial x^2} + \frac{\partial^2 u}{\partial y^2} + \frac{\partial^2 u}{\partial z^2}) \qquad (2)$$

$$u\frac{\partial v}{\partial x} + v\frac{\partial v}{\partial y} + w\frac{\partial v}{\partial z} = -\frac{1}{\rho}\frac{\partial \rho}{\partial y} + \frac{\mu}{\rho}\left(\frac{\partial^2 v}{\partial x^2} + \frac{\partial^2 v}{\partial y^2} + \frac{\partial^2 v}{\partial z^2}\right) \qquad (3)$$

$$u\frac{\partial w}{\partial x} + v\frac{\partial w}{\partial y} + w\frac{\partial w}{\partial z} = -\frac{1}{\rho}\frac{\partial \rho}{\partial z} + \frac{\mu}{\rho}(\frac{\partial^2 w}{\partial x^2} + \frac{\partial^2 w}{\partial y^2} + \frac{\partial^2 w}{\partial z^2}) \qquad (4)$$

Energy equation:

$$\rho Cp\left(u\frac{\partial He}{\partial x} + v\frac{\partial He}{\partial y} + w\frac{\partial He}{\partial z}\right) = k\left(\frac{\partial^2 T}{\partial x^2} + \frac{\partial^2 T}{\partial y^2} + \frac{\partial^2 T}{\partial z^2}\right) \qquad (5)$$

Equation (6) describes the enthalpy suspension (He), which can be computed by adding the sensible heat (he) and latent heat (ΔH) of PCM

$$He = he + \Delta H \qquad (6)$$

Eq. (7) describes sensible heat:

$$he = h_{ref.} + \int_{T_{ref.}}^{T} Cp_F \, dt \qquad (7)$$

where: $h_{ref.}$ Enthalpy at $T_{ref.}$ reference

As a function of the molten mass fraction (β), fusion latent heat of PCM (L) MEPCM mass fraction (ϕ), Eq (8) defines slurry latent heat (ΔH). PCM molten mass ratio slurry is known as the molten mass fraction (β). The PCM begins to melt at $T_{solidus}$ and finishing melting $T_{liquids}$, varying from 0 at $T_{solidus}$ to 1 at $T_{liquids}$ Eq. (9), represent the molten mass fraction (β).

$$\Delta H = \beta L \varphi \qquad (8)$$
where:

$$\beta = 0 \qquad\qquad if \qquad T_f < T_{solidus}$$

$$\beta = 1 \qquad\qquad if \qquad T_f > T_{liquids}$$

$$\beta = \frac{T_f - T_{solidus}}{T_f - T_{liquids}} \qquad if \qquad T_{solidus} < T_f < T_{liquids} \qquad (9)$$

The density of PCMs was calculated from this relationship and taken the mean of its liquid and solid densities.

$$\rho_{PCM} = \frac{10}{7} \left(\frac{d_c}{d_{PCM}}\right)^3 \rho_C \qquad (10)$$

$$C_{PPCM=} \frac{(7Cp_c + 3 Cp_{wall})\rho_c \rho_{wall}}{(3 \rho c + 7 \rho_{wall})\rho_{PCM}} \qquad (11)$$

Thermal conductivity of the microcapsules calculated by using multipart of sphere approach:

$$\frac{1}{K_{PCM} \, d_{PCM}} = \frac{1}{K_C \, d_c} + \frac{d_{PCM} - d_c}{K_{wall} \, d_{PCM} \, d_c} \qquad (12)$$

5.2 Properties of Suspension

The properties of suspension are a grouping of the properties of suspending fluid and microcapsules. The density and specific heat are calculated by using mass and energy balance (Socaciu, 2012).

$$\rho_f = (1 - Cp)\rho_W + Cp_{PCM} \qquad (13)$$

$$C_{PF} = (1 - \varphi)Cp_w + \varphi Cp_{PCM} \qquad (14)$$

The mass fraction (φ), the viscosity of the suspension (μ_f) and (C) volumetric concentration (%) were calculated from the following equations:

$$\varphi = \frac{C\rho_{PCM}}{(\rho_w + C(\rho_{PCM} - \rho_w))} = \frac{C\rho_{PCM}}{\rho_f} \qquad (15)$$

$$\mu_f = \mu_w(1 - C - 1.16 \, C^2)^{-2.5} \qquad (16)$$

This relationship has been found to be functional for concentration as high as 20%, mean element diameter ranging from (0.3 – 400) μm and a diameter –to-particle ratio of (20 – 100).

The thermal conductivity of suspension(K_f) was calculated from the following relationship:

$$K_f = \frac{2k_w + k_{PCM} + 2 C \left(K_{pcm} - k_w\right)}{2 + \frac{K_{PCM}}{k_w} - C \left(\frac{k_{PCM}}{K_w} - 1\right)} \qquad (17)$$

The thermal performance of heat sink is represented by a heat transferred rate and Nusselt number which are calculated by:

$$q = m^. C_p \left(T_{fin} - T_{fo}\right) \qquad (18)$$

$$Nu = \frac{h \, L}{K_f} \qquad (19)$$

And to obtain a performance index providing information about the heat sink's overall performance is used which represented the ratio of heat transferred (q) to the pumping power (p.p) required which calculated from this relationship:

$$\eta = \frac{q}{p.p} \qquad (20)$$

Where: $p.p = \Delta p.V^.$ (21)
pressure drop is equivalent to:
$\Delta p = p_{fout} - p_{fin}$ (22)
Flow rate is equivalent to:
$V^. = A.v$ (23)

MEPCM suspension is examined in this work at the following concentrations: 2%, 5%, 10%, 15%, and 20%. Table 1 list the material's thermo-physical characteristics of materials studied (Climates et al., 2013), (KENISARIN & MAHKAMOV, 2007).

Table 1: suspension components physical properties

NO	Materials	$\rho(kg/m3)$	Cp(J/kg K)	K(W/m K)	μ(kg/m s)
1	Pure water	981.3	4189	0.643	0.000598
2	Ethylene glycol	1111.4	2415	0.254	0.0157
3	Transformer oil	870	2000	0.109	0.0124
4	(PCM) RT44	771	2000	0.2	_
5	(PCM)N-octadecane	S = 850, L= 780	2222	0.358	_
6	(MEPCM wall) PMMA	1190	1470	0.21	_
7	(MEPCM wall) PAO	783	2242	0.143	_

6   Numerical Solution

The system of boundary conditions and governing equations above is numerically solved using the finite volume method (FVM). The numerical model has been solved using Computational fluid dynamics (CFD) model. In this studied CFD software FLUENT 6.3 is employed in the present model's solution. The SIMPLE algorithm is employed in order to computing the flow variables and solve the problem of coupling of velocity and pressure. Size recognition of grid is used to choose the mesh for this system's solution grid so that to find suitable size of mesh, a mesh refinement has been made that give a highly accurate answer. Table 2 lists the various meshes that were selected. The fourth mesh will be used for all next solutions because of the solution becomes independent of mesh size after the fourth mesh as can be seen in this table.
The requirements for convergence that govern the energy and momentum equation solutions is 10^{-6}.

Table 2: Mesh Independence study

NO	Mesh dimensions	Outlet temperature (K)
1	Mesh1 (interval size = 0.0005)	314.5
2	Mesh2 (interval size = 0.0004)	314.6
3	Mesh3 (interval size = 0.0003)	314.78
4	Mesh4 (interval size = 0.0002)	314.17
5	Mesh5 (interval size = 0.00015)	314.02
6	Mesh6 (interval size = 0.0001)	314

6.1   Boundary conditions

The mathematical model is closed by applying the following boundary conditions:
1. No slip at the wall; u = v = w = 0.
2. Steady flow of heat at the lower wall = 640 W/m^2, inlet velocity (0.28 m/s) and inlet temperature T=25 C°.

3. Symmetry B.C at the left and right of micro heat sink.
4. Fully developed flow at the channel's end.
5. No slip combination transfers heat at the interface of a fluid and a solid.

7 Results and Discussions

7.1 Validation

To check the validity of used numerical model, this model is validated with numerical model presented in (Sabbah et al., 2009). The numerical model of micro-channel heat with a vertical height 1.5 mm, a length 10mm and a width 5.1mm is presented in (Sabbah et al., 2009). The volume fraction of MEPCM Analysis is carried out on water slurry are analyzed at 0% (pure water), 5%, 10%, 15%, 20%, and 25%.

In this investigation, the temperature was recorded at the heat sink's base under specific boundary conditions. These conditions included varying the inlet temperature to 25C°, a heat flux constant at (100 W/cm^2), and an inlet velocity of 1 m/s applied at the bottom wall for each of the various design models. In order to prevent communication during validation, this result was also, limited to pure water at a concentration 0% and ignored rest concentrations.

The numerical results of researcher (Sabbah et al., 2009) and the current model's results of the temperature along heat sink's bottom wall are compared in figure 3. This figure shows that, when the maximum error is 0.96%, there is acceptable agreement between the results.
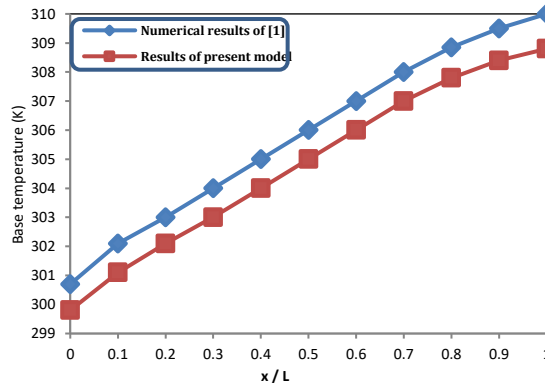
Figure 3: Base temperature variation along a micro-channel heat sink as a comparison of the outcomes of (Sabbah et al., 2009) of present model for pure water

7.2 Results

Figures (4, 5, and 6) show the variation of base temperature (Ө), where Ө = ((Tb-Tin)/(Tin-Tout)) with ambient temperature for un-finned heat sink and a heat sink with fins (circular, triangular and square) for different coolants fluid (pure water, ethyleneglycol and pure oil) at constant inlet velocity (0.28 m/s), different inlet temperature and heat flux applied (640 W/m^2). From these figures it can be noted that, base temperature increased with ambient temperature for every pure fluids utilized as a result of a decline in amount of the difference of temperature between inlet and outlet of the channel. The results also show that the base temperature dropped when fins were used in place of an un-finned heat sink and that the circular fins produced a lower temperature than the other fins types. Additionally, because of the characteristics of water and its high specific heat, Figure 4 shows a lower temperature for pure water when compared to other figures.
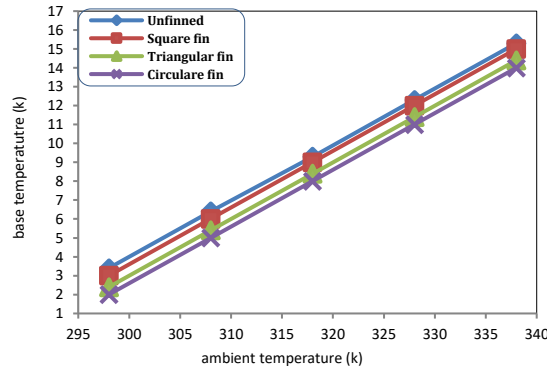
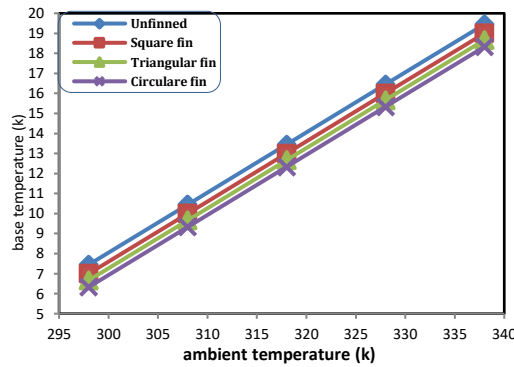Figure 4: Base temperature change for pure water with respect to ambient temperature

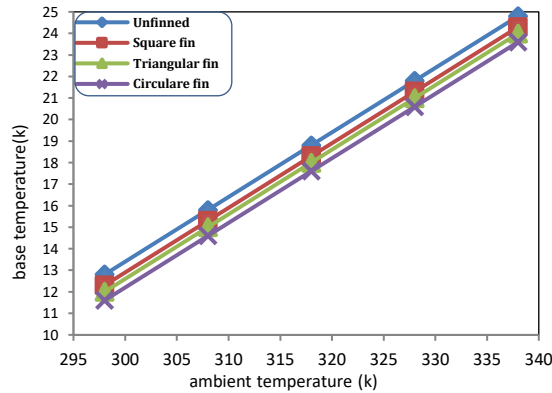Figure 5: Base temperature variation for ethyleneglycol with ambient temperature

Figure 6: Base temperature variation for pure oil with ambient temperature

Figures (7, 8 and 9) display the variation of base temperature (Ө), where Ө = ((Tb-Tin)/(Tin-Tout)) with ambient temperature for unfinned heat sink and a heat sink with fins (circular, triangular and square) for different coolants fluid represented with (Air, RT44 and n-octadecane) at heat flux applied on the base of heat sink (640 W/m^2). From these figures it can be illustrious that, base temperature, increased with ambient temperature for all coolants fluid used. From these figures it can be seen that, circular fins gives lower temperature related with unfinned and others fins used. Also, the Figure 9 gives lower temperature for (n-octadecane) compared with other figures due to properties of PCM used. That is because of melting temperature for (n-octa.) lower than the melting temperature for (RT44).
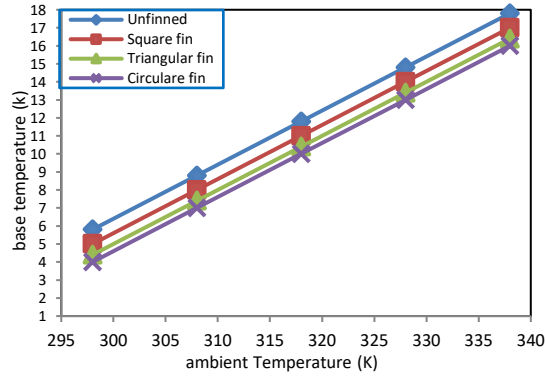
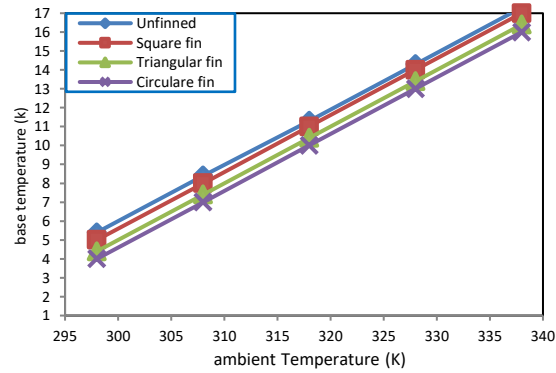Figure 7: Base temperature variation for pure air with ambient temperature

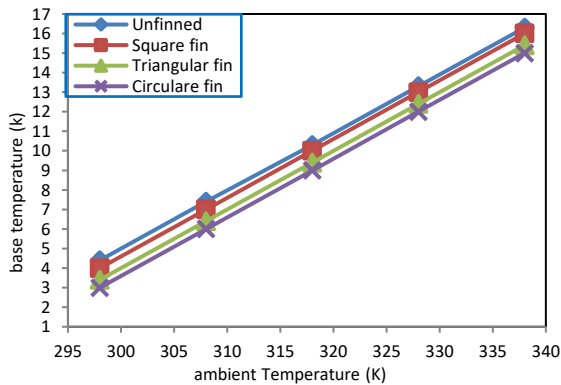Figure 8: Base temperature variation for (RT44) with ambient temperature

Figure 9: Base temperature variation for (n-octad.) with ambient temperature

Figures (10 and 11) indicate the variation of base temperature (Θ), where $\Theta = ((Tb-Tin)/(Tin-Tout))$ utilizing the Reynolds number for unfinned heat sink and a heat sink that has (circular, triangular, and square) fins for different MEPCM suspensions consist of pure water and different combinations of PCM and wall materials at concentration 20%. Figure 10 reveal that the suspension consists of (RT44) with PMMA and pure water with unfinned and finned heat sink give lower temperature due to properties of its components (RT44 and PMMA).
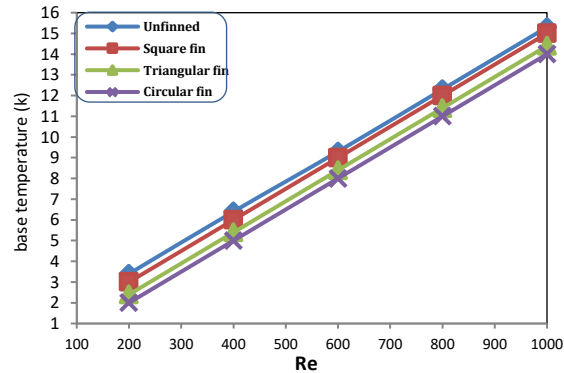
Figure 10: Base temperature variation with Reynolds number for 20% concentration water-based (RT44+PMMA) suspension
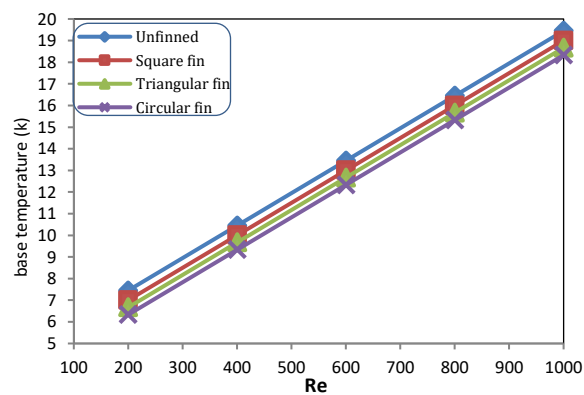

Figure 11: Base temperature variation with Reynolds number for 20% concentration water-based (RT44+PAO) suspension

Figures (12 and 13) show the variation of base temperature (Ɵ), where Ɵ = ((Tb-Tin)/(Tin-Tout)) utilizing the Reynolds number for unfinned heat sink and a heat sink that has (circular, triangular, and square) fins for different MEPCM suspensions consist of pure water and different combinations of PCM and wall materials at concentration at 20%. Figure 12 reveal that the suspension consists of (n-octadecane) with PMMA and pure water with unfinned and finned heat sink give lower temperature due to good properties of its components (n-octadecane and PMMA) where (n-octadecane) have higher fusion's latent heat and PMMA have higher thermal conductivity.

From all figures above it can be observe that, Ɵ increased with increasing the Reynolds number for all MEPCM suspensions due to decreased in temperature difference and the heat transferred amount from a heat sink as a results of increasing flow velocity. From two figures demonstrate that, in all cases of unfinned heat sink give high temperature compared with others fins. However, the square and triangular fins raise temperature, while, circular fins reduce it due to increasing in surface exchange area and heat transfer from fins in regular shape in all directions.
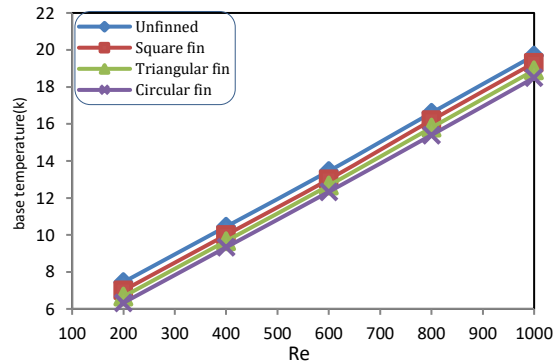
Figure 12: Base temperature variation with Reynolds number for 20% concentration water-based (n-octa.+PMMA) suspension
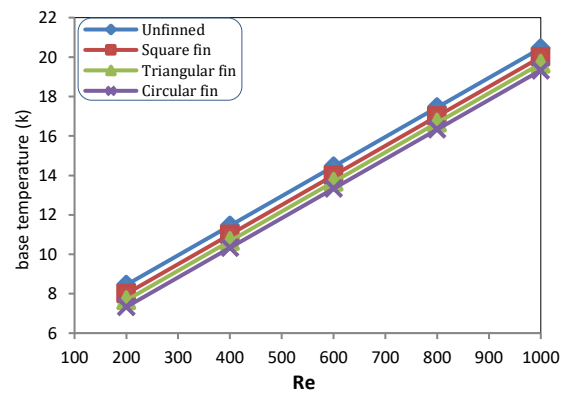

Figure 13: Base temperature variation with Reynolds number for 20% concentration water-based (n-octa.+PAO) suspension

The total pressure drop's variation with a Reynolds number for unfinned heat sink and a heat sink equipped with (square, triangular, and circular) fins when the volume between the fins filled with MEPCM suspension for a concentration 2% is presented in Figure 14. In this illustration used (n-octadecane) PMMA (MEPCM wall) and MEPCM core for pure water at concentration 2% due to this concentration gives a lower pressure drop. It is evident from this figure that, As the Reynolds number increased, the pressure dropped as well and unfinned heat sink gives a lower pressure drop and square fins give high pressure drops compare with other types of fins used.
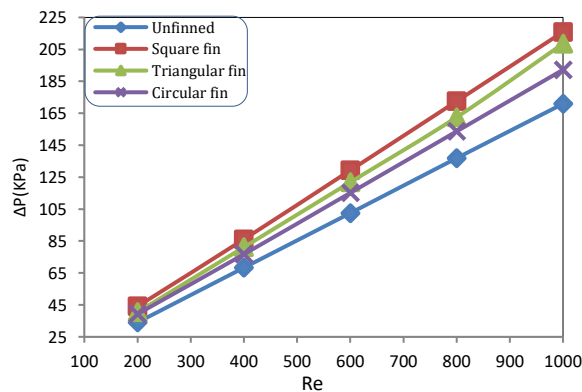

Figure 14: Pressure drop variation with Reynolds number for 2% concentration water-based (n-octa.+PMMA) suspension

Figure 15 display total pressure drop's variation with a Reynolds number for unfinned and finned heat sink equipped with (square, triangular, and circular) when the volume between the fins filled with PCM (n-octadecane). It is evident from this figure that, square fins give high pressure drop's while unfinned heat sink gives a lower pressure drop. Additionally, as the Reynolds number increased, so did the total pressure drop.
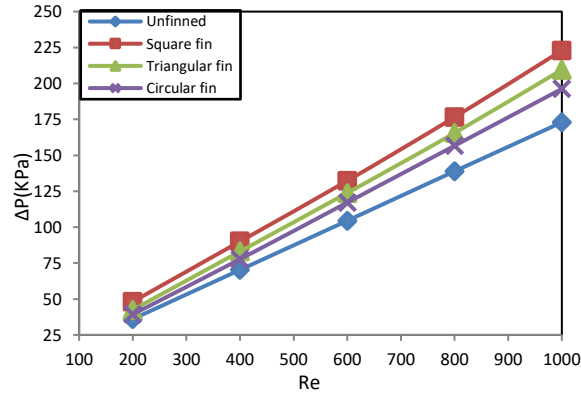

Figure 15: Pressure drop variation with Reynolds number for (n-octa.)

Figure 16 express the heat sink's performance factor variation with Reynolds number for unfinned heat sink and heat sink equipped with fins (square, triangular, and circular). Suspension consists of (n-octadecane) with PMMA and pure oil with unfinned and finned heat sink at concentration 2%. This figure clearly shows that, (n-octadecane) with PMMA and pure oil give high performance due to the properties of these materials (n-octadecane and PMMA) where (n-octadecane) have higher latent heat of fusion and PMMA have higher thermal conductivity. Also, in all figures its can be predictable that, the unfinned heat sink give high performance due to high heat transfer coefficient and lower pressure drop for unfinned heat sink and the circular fins give high performance compared with others fins used.
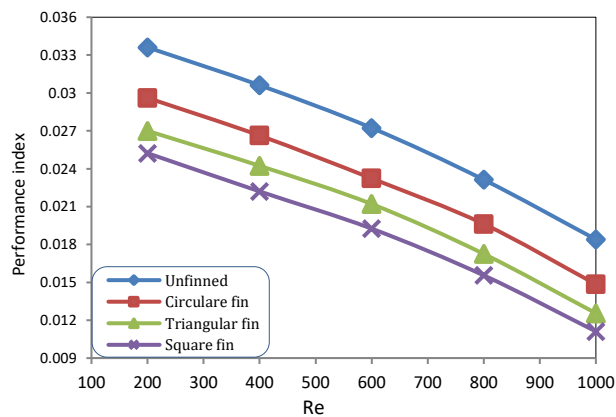

Figure 16: performance factor variation with Reynolds number for a suspension pure oil based (n-octa.+PMMA) at concentration 2%

Figure 17 display the variation of performance factor with Reynolds number for unfinned and finned heat sink equipped with fins (square, triangular, and circular) fins. This figure shows that as the Reynolds number increased, the heat sink's performance decreased. Because of the properties of PCM (n-octa.), where fusion latent heat is higher. Also, the performance factor for circular fins higher from square, and triangular fins. Furthermore, its can be predictable that, the unfinned heat sink give high performance due to high heat transfer coefficient and lower pressure drop for unfinned heat sink and the circular fins give high performance compared with others fins.
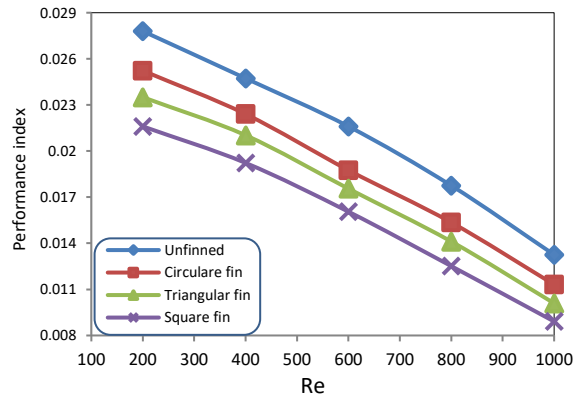

Figure 17: Performance factor variation with Reynolds number for (n-octa.)

8   Conclusions

The conclusions it is can be obtained from the results above:
1. The PCM (n-octa.) gives lower temperature with ambient temperature compared with (RT44).
2. MEPCM suspension consists of (n-octa.) with PMMA gives lower temperature and higher performance compared with all pure fluids and suspension used.
3. Using of MEPCMs and PCMs in heat sink leads to reduce heat sink temperature compared with cases using only air, pure water, Ethylene glycol, and pure oil.
4. Unfinned heat sink gives lower pressure drop and high rate of heat transfer coefficient compared with all types of fins used.
5. Pure oil based MEPCM suspension gives higher performance compare with MEPCM suspension of ethyleneglycol and pure water and pure air based PCM.
6. When used MEPCM suspension with unfinned heat sink are given high performance in all cases compared with others fins therefore this preferred unfinned for design facilities side, cost and expenditure is lower from design any types of fins.

9   References

Agrawal, N., & Dewangan, M. (2013). Heat Transfer Analysis of Micro Channel Heat Sink. International Journal of Science and Research, ISSN, 2319–7064.

Arshad, A., Ali, H. M., Khushnood, S., & Jabbal, M. (2018). Experimental investigation of PCM based round pin-fin heat sinks for thermal management of electronics: Effect of pin-fin diameter. International Journal of Heat and Mass Transfer, 117, 861–872. https://doi.org/10.1016/j.ijheatmasstransfer.2017.10.008

Arshad, A., Ali, H. M., Yan, W.-M., Hussein, A. K., & Ahmadlouydarab, M. (2018). An experimental study of enhanced heat sinks for thermal management using n-eicosane as phase change material. Applied Thermal Engineering, 132, 52–66. https://doi.org/10.1016/j.applthermaleng.2017.12.066

Climates, S. U. S., Kosny, J., Shukla, N., & Fallahi, A. (2013). Cost Analysis of Simple Phase Change Material-Enhanced Building Envelopes in. January. http://www.nrel.gov/docs/fy13osti/55553.pdf

Fayyaz, H., Hussain, A., Ali, I., Shahid, H., & Ali, H. M. (2022). Experimental Analysis of Nano-Enhanced Phase-Change Material with Different Configurations of Heat Sinks. Materials, 15(22), 8244. https://doi.org/10.3390/ma15228244

Hasan, M. I. (2016). Study of microchannel heat sink performance with expanded microchannels and nanofluid. Journal of Al-Qadisiya for Engineer Sciences, 9(4), 526–542.

Hasan, M. I., & Tbena, H. L. (2018). Using of phase change materials to enhance the thermal performance of micro channel heat sink. Engineering Science and Technology, an International Journal, 21(3), 517–526. https://doi.org/10.1016/j.jestch.2018.03.017

KENISARIN, M., & MAHKAMOV, K. (2007). Solar energy storage using phase change materials☆. Renewable and Sustainable Energy Reviews, 11(9), 1913–1965. https://doi.org/10.1016/j.rser.2006.05.005

Mehravar, S., & Sabbaghi, S. (2014). Thermal Performance of MEMS-Based Heat Exchanger with Micro-Encapsulated PCM Slurry. Journal of Power and Energy Engineering, 02(09), 15–22. https://doi.org/10.4236/jpee.2014.29003

Sabbah, R., Farid, M. M., & Al-Hallaj, S. (2009). Micro-channel heat sink with slurry of water with micro-encapsulated phase change material: 3D-numerical study. Applied Thermal Engineering, 29(2–3), 445–454. https://doi.org/10.1016/j.applthermaleng.2008.03.027

Socaciu, L. G. (2012). Thermal energy storage with phase change material. Leonardo Electronic Journal of Practices and Technologies, 11(20), 75–98. https://doi.org/10.1201/9780367567699

Soodphakdee, D., Behnia, M., & Copeland, D. (2001). A comparison of fin geometries for heatsinks in laminar forced convection: Part I-round, elliptical, and plate fins in staggered and in-line configurations. The International Journal of Microcircuits and Electronic Packaging, 24(1), 68–76. http://www.imaps.org/journal/2001/Q1/soodphakdee-1.pdf